Video Article

Imaging Ca^{2+} Dynamics in Cone Photoreceptor Axon Terminals of the Mouse Retina

Manoj Kulkarni[1,2], Timm Schubert[1,3], Tom Baden[1,2,3], Bernd Wissinger[4,5], Thomas Euler[1,2,3], Francois Paquet-Durand[1]

[1]Institute for Ophthalmic Research, University of Tübingen

[2]Graduate School of Cellular & Molecular Neuroscience, University of Tübingen

[3]Bernstein Centre for Computational Neuroscience, University of Tübingen

[4]Molecular Genetics Laboratory, University of Tübingen

[5]Centre for Ophthalmology, University of Tübingen

Correspondence to: Thomas Euler at thomas.euler@cin.uni-tuebingen.de, Francois Paquet-Durand at francois.paquet-durand@klinikum.uni-tuebingen.de

Abstract

Retinal cone photoreceptors (cones) serve daylight vision and are the basis of color discrimination. They are subject to degeneration, often leading to blindness in many retinal diseases. Calcium (Ca^{2+}), a key second messenger in photoreceptor signaling and metabolism, has been proposed to be indirectly linked with photoreceptor degeneration in various animal models. Systematically studying these aspects of cone physiology and pathophysiology has been hampered by the difficulties of electrically recording from these small cells, in particular in the mouse where the retina is dominated by rod photoreceptors. To circumvent this issue, we established a two-photon Ca^{2+} imaging protocol using a transgenic mouse line that expresses the genetically encoded Ca^{2+} biosensor TN-XL exclusively in cones and can be crossbred with mouse models for photoreceptor degeneration. The protocol described here involves preparing vertical sections ("slices") of retinas from mice and optical imaging of light stimulus-evoked changes in cone Ca^{2+} level. The protocol also allows "in-slice measurement" of absolute Ca^{2+} concentrations; as the recordings can be followed by calibration. This protocol enables studies into functional cone properties and is expected to contribute to the understanding of cone Ca^{2+} signaling as well as the potential involvement of Ca^{2+} in photoreceptor death and retinal degeneration.

Video Link

The video component of this article can be found at https://www.jove.com/video/52588/

Introduction

Vision begins with the light-induced activation of the phototransduction cascade in retinal photoreceptors. Rod photoreceptors allow vision at low light levels, whereas cone photoreceptors mediate colour and high-resolution daylight vision. Many photoreceptor-specific genes are susceptible to mutations that lead to degeneration of these cells. A number of molecular markers associated with photoreceptor loss have been identified[1], but so far the detailed molecular mechanisms and the sequence of events remain unclear. Altered Ca^{2+} homeostasis was speculated to be a trigger of photoreceptor cell death, a hypothesis supported by the up-regulation of the activity of Ca^{2+}-dependent calpain-type proteases during the degeneration process[2,3]. However, to date, this hypothesis is not backed by physiological measurements of Ca^{2+}. Inconsistencies in several studies on the effect of Ca^{2+} channel blockers in retinal diseases further challenged the involvement of Ca^{2+} in cell death[4-6], calling for methods to directly assess Ca^{2+} in mammalian cone photoreceptors.

Previously, most electrical recording and Ca^{2+} imaging studies have been performed in amphibian and reptilian models because of the easier access to cones[7-9]. However, mammalian photoreceptor physiology may be different from that of non-mammals[10] and especially, in the context of human hereditary retinal degeneration, a better understanding of mammalian photoreceptor physiology is a key to the development of innovative treatments. Many mouse models mimicking human retinal diseases are available but little is known about Ca^{2+} dynamics in mouse cones[11]. Electrical techniques are not suitable for high-throughput recordings from cones, in particular not in mice, where rods (~97%) significantly outnumber cones (~3%)[12]. Moreover, sensitive electrophysiological techniques such as whole-cell patch-clamp recordings disturb the intracellular milieu and provide data on Ca^{2+} currents but not on absolute intracellular Ca^{2+} concentrations. Hence, despite the lower temporal resolution, imaging is the method of choice when addressing questions about cone Ca^{2+} dynamics. The key issue with imaging is how to selectively label the cones with a fluorescent Ca^{2+} indicator dye. Proper compartmentalization and cell specificity is hard to achieve by "bulk-loading" synthetic Ca^{2+} indicator dyes into the tissue. As a consequence, labelled cones, rods[13,14], and Müller glial cells cannot be reliably distinguished. Also, synthetic dyes tend to leak out of the cells, preventing prolonged recordings under consistent conditions. Furthermore, loading synthetic Ca^{2+} indicators in their AM-ester form is problematic, as it requires detergents (*e.g.,* DMSO) and generates formaldehyde[15]. For

absolute Ca^{2+} measurements, ratiometric indicators are mandatory. However, the best currently available synthetic ratiometric indicator Fura-2 requires excitation light in the range of 700 to 760 nm (for two-photon excitation), which, depending on its intensity, can in itself stimulate the cones, and thus impede studies of cone Ca^{2+} dynamics under physiological illumination conditions.

Unlike synthetic dyes, genetically-encoded Ca^{2+} indicators can be expressed in a cell type-selective manner. They do not leak out of cells, and therefore, if bleaching is avoided, prolonged and reliable ratiometric measurements are possible. Cell type-selective expression of Ca^{2+} biosensors, when combined with two-photon microscopy, represents a powerful tool to assess and study subcellular Ca^{2+} under largely physiological conditions[13,16,17]. Here, we describe a protocol to study light stimulus-evoked cone Ca^{2+} dynamics in a transgenic Ca^{2+} biosensor mouse line (HR2.1:TN-XL), which expresses the FRET-based Ca^{2+} biosensor TN-XL[18] selectively in cones, under the human red opsin promoter HR2.1[19]. To access the cone terminals, an *ex-vivo* slice preparation[20] was employed. The protocol was already successfully used in three studies on cone function in healthy mice[10,21,22]. Moreover, the protocol allows studying cone Ca^{2+} signaling in specific genetic conditions, *e.g.,* by crossbreeding mouse models for hereditary retinal degeneration with HR2.1:TN-XL mice.

Protocol

All animal procedures were carried out adhering to the guidelines and laws for animal protection determined by German Federal Government and approved by the institutional animal welfare committee of the University of Tübingen.

1. Animal Models

1. HR2.1:TN-XL Ca^{2+} biosensor mouse
   1. Use the transgenic HR2.1:TN-XL mouse line expressing the Ca^{2+} biosensor TN-XL selectively in cone photoreceptors[10]. Use 3 - 6 weeks old mice of either sex raised with a standard 12 hrs day/night rhythm.

2. Retinal Dissection

1. Physiological solution
   1. Prepare freshly 2 L of extracellular solution, containing 125 mM NaCl, 2.5 mM KCl, 1 mM $MgCl_2$, 1.25 mM NaH_2PO_4, 26 mM $NaHCO_3$, 0.5 mM L-glutamine, and 20 mM (+) glucose. Mix until all ingredients dissolve.
   2. "Bubble" extracellular solution with carboxygen (95% O_2, 5% CO_2) for 5 - 10 min. Add $CaCl_2$ to reach a concentration of 2 mM.
   3. After bubbling the extracellular solution, measure its pH. The pH should be 7.4, otherwise it is likely that mistakes have been made during the preparation of the solution. Keep bubbling rate and solution temperature constant throughout experiment to ensure constant pH.
   4. Separate the stock into 2 flasks, one for retina dissection and one for the recording setup (perfusion).

2. Eye enucleation and isolation of retina (5 - 10 min)
   1. Maintain a dim red illumination in the working area for enucleation. Use LEDs with a peak wavelength of 650 nm (or longer) to avoid bleaching of cones during dissection.
   2. Dark-adapt the mouse for 2 hrs by putting its cage into a well-ventilated, lightproof box to ensure that cones are fully sensitized at time of recordings.
   3. Anaesthetize the mouse under a laboratory hood with isoflurane (5%) using a vaporizer and a gas-tight container that holds a standard mouse cage. Carefully follow the manufacturer´s instructions when handling the vaporizer. Use gloves and face mask to reduce exposure to allergens.
   4. Use a binocular microscope with a 10 - 40X magnification for dissection.
   5. Sacrifice the anaesthetized mouse by decapitation.
   6. For orientation, mark the top of each eye (= dorsal) with a waterproof pen. Keep track on whether using left or right eye.
   7. Remove the eye carefully using curved scissors by cutting the optic nerve behind the eyeball. For dissection, transfer the eyeball to a Petri dish containing freshly carboxygenated extracellular solution. For transferring the eyeball, hold it by the optic nerve stump.
   8. Pierce the eye at any point along the border between the cornea and the sclera (*i.e.,* at the *ora serrata*) with a sharp injection needle.
   9. Hold the eye at the sclera with a pair of forceps and gently insert one scissors blade into the hole made in the previous step. Cut along the *ora serrata* to separate the anterior part of the eye (cornea, lens, vitreous body) from the posterior part (eyecup). Cut the eyecup radially (towards the optic disc) at the position of the pen mark to indicate the dorsal position on the retina.
      Note: Prepared this way, the eyecups can be kept in constantly carboxygenated solution for later use.
   10. Turn the eyecup in the Petri dish such that the dorsal cut points away from oneself. Grab the sclera on the left and the right side of the eyecup with a pair of forceps each by inserting the forceps tips between retina and sclera.
   11. Detach the retina by gently inverting the scleral part of the eyecup. Finally, cut the optic nerve using micro dissecting scissors to free the retina from the sclera.
       Note: This is a critical step. Avoid damage to the retina (*e.g.,* by touching and squeezing it with forceps).
   12. Hold one of the edges of the retina with a pair of forceps and gently remove debris and vitreous body from the retinal surface using a second pair of forceps. When the retinal surface is clean, use micro dissecting scissors to make three additional shorter, radial cuts (approximately every 90°). These cuts allow one to carefully flatten the retina with the photoreceptor side facing down in the Petri dish (**Figure 1A**).

3. Slice preparation (10 - 15 min)
   1. Prepare beforehand nitrocellulose filter membranes for retinal slicing and glass cover-slips for mounting slices and transferring them to the recording chamber. Cut nitrocellulose filter membrane into approximately 10 x 5 mm sized rectangular pieces using scissors. Cut coverslips into approximately 10 x 5 mm sized rectangular pieces using a glasscutter.

2. Slowly immerse a glass slide into the extracellular solution close to tissue. Gently, pull the retina onto the glass slide with the ganglion cell side up by grabbing it at the very edge using a pair of forceps. This process reduces mechanical damage and folding of tissue.
3. Choose the region of the retina that is related to the respective research question (see also Discussion). Remember, the long cut made in step 2.2.9 marks the dorsal retinal half (**Figure 1A**). Cut a rectangular, approximately 1 x 2 mm sized piece out of the selected retinal region using a curved scalpel blade. Wipe off excess solution around the tissue.
4. Place the filter membrane on top of the piece of retina such that the ganglion cell side adheres to the membrane. Immediately, add a drop of extracellular medium onto the membrane to firmly attach the tissue to the membrane.
5. Transfer the membrane-mounted retinal tissue to the slicing chamber containing fresh extracellular solution.
6. Cut retina into vertical slices of 200 µm thickness (**Figure 1B**) using a fresh razor blade attached to a tissue chopper[23]. Change blade for every retinal piece.
   Note: The razor blade needs to be perfectly aligned with the surface of the slicing chamber bottom such that the whole membrane splits simultaneously, as indicated by a "clicking" sound when cutting – otherwise the blade may bend and damage the slice.
7. Glue a single membrane-mounted slice to a glass cover-slip by applying high vacuum grease to the membrane ends only (**Figure 1C**). Keep the glass surface below the retina free from grease.
8. Keep coverslip-mounted slices covered by a drop of extracellular solution in the holding chamber – a closed and lightproof container, *e.g.,* a Petri dish with the lid covered with aluminium foil – under a carboxygen atmosphere at RT. Introduce carboxygen by bubbling a small water reservoir to keep the atmosphere in the holding chamber humidified; this prevents the slices from drying out.
9. Allow slices to rest in the holding chamber for 10 - 15 min before moving them (one by one) to the recording chamber. Slices can be maintained up to 4-5 hrs in holding chamber at RT (~21 °C).

3. Two-photon Ca^{2+} Imaging

1. Two-photon microscopy
   1. Use a Movable Objective Microscope (MOM)-type two-photon microscope. Both MOM design and imaging procedures were described earlier[24], for details see also[10,21,25] (for sources and companies, see **Table 1**).
      Note: Any upright two-photon microscope that fulfils the following minimal requirements can be used: It has to be equipped with (*a*) a pulsed laser tuneable to ~860 nm, (*b*) a minimum of two simultaneously acquired fluorescence channels, (*c*) filters for eCFP and citrine fluorescence, (*d*) a light stimulator (for possible designs, see[24,26]), and (*e*) software that allows recording time-lapsed image sequences at a frame rate sufficient to resolve the Ca^{2+} signals of interest.
   2. Start the two-photon imaging system as indicated by the manufacturer. Strictly follow the facility's laser safety guidelines. Start the laser and tune it to ~860 nm.
   3. Transfer a slice from the holding chamber to the recording chamber and immediately start perfusing with carboxygenated extracellular solution. Maintain a perfusion flow rate of 2 ml/min and a temperature of 37 °C in the recording chamber.
   4. Use a 20X 0.95 NA water immersion objective. If available, use a CCD camera in combination with an infra-red LED below recording chamber to locate the retinal slice (**Figure 2**). Otherwise locate slice using two-photon imaging (see 3.1.5).
   5. Switch to two-photon imaging to view biosensor expression. Turn on the two detection channels for fluorescence imaging of eCFP and citrine.
   6. Use the image acquisition software that controls the two-photon microscope to scan and select a row of cone terminals for recording (**Figure 3A**). Set image acquisition to 128 x 16 pixel images (31.25 Hz) or a similar configuration. Restrict scanned area to cone terminals to avoid bleaching of photopigments in outer segments.
      Note: For the TN-XL calcium sensor (τ = ~0.6 sec for Ca^{2+} binding, τ = ~0.2 sec for Ca^{2+} unbinding; see[16]) a minimum frame rate of ~8 Hz is recommended.

2. Light stimulation and recording
   1. Use a sub-stage full-field light stimulator as described elsewhere[10,21,26] to perform the following steps.
      Note: A simple solution for a full-field light stimulator is to use two band-pass-filtered LEDs (*e.g.,* "blue": 360 BP 12, "green": 578 BP 10) that match the wavelength sensitivities of mouse cones but at the same time do not overlap with the filters used for fluorescence detection (*cf.* 3.2.4). The light from the LEDs is focused by the condenser through the bottom of the recording chamber (**Figure 2**). For details on this stimulator design, its calibration, the light intensities used and the evoked cone photo-isomerisation rates, see[10,21,26].
   2. Turn on the laser and allow cones to adapt to the scanning laser and the stimulus background light (20 - 30 sec, see also Potential Pitfalls) before presenting light stimuli (see 3.2.3) or applying pharmacological agents.
   3. Start presentation of arbitrary stimuli (*e.g.,* flashes of light, as shown in **Figure 3B,C**). In the case of the stimulator described in step 3.2.1, generate the stimuli by modulating the intensity of the two LEDs over time using a microprocessor board controlled by customized software (for details, see[10,21,26]).
   4. Start recording the two fluorescence channels (*e.g.,* at 483 nm for "blue" FRET-donor eCFP and at 535 nm for "yellow" FRET-acceptor; for specs see **Table 1**) simultaneously using the respective image acquisition software (see also 3.1.6). For example, in the case of light flashes (**Figure 3B,C**), record at least 8 - 10 stimulus presentations (trials).

3. "In-slice" Ca^{2+} calibration
   1. Record Ca^{2+} signals in cone terminals (as described in 3.1.6 and 3.2.4) and extract the baseline Ca^{2+} level in a set of cones (as described in 3.4).
   2. Switch to "Ca^{2+} free" extracellular medium with 5 µM ionomycin (dissolved in DMSO) and 10 mM EGTA (or, alternatively, BAPTA) added. Record cone terminals again every 5 min to determine the minimal fluorescence ratio (R_{min}), *i.e.,* the ratio in the (near) absence of intracellular Ca^{2+}. This may take anywhere between 15 - 30 min.
      Note: A perfusion system is required that allows switching between different reservoirs.
   3. Switch to extracellular medium with 5 µM ionomycin (dissolved in DMSO) and 2.5 mM Ca^{2+}. After an incubation time of 5 min, record cones again every 5 min to measure the maximal fluorescence ratio (R_{max}), *i.e.,* the ratio in the presence of saturating concentrations of intracellular Ca^{2+}. Following ionomycin application, it may take between 3 - 15 min for the Ca^{2+} ratio to become stable.

Note: Exposing the slices to high Ca^{2+} and ionomycin for a longer period will eventually damage the cells. Include only cells in the analysis that retain their normal morphology. Concentrations (*i.e.,* EGTA, ionomycin) may need to be adapted. For more details on the Ca^{2+} calibration protocol, see[13,17].

4. Data analysis
   Note: Use an image processing and data analysis software package compatible with the respective microscope software and capable of running custom analysis scripts.

   1. Load an imaging data file and draw regions of interest (ROIs) around each cone terminal (**Figure 3A**). For each frame, average fluorescence intensity within the ROI and subtract background fluorescence, before calculating the ratio (R) between FRET-acceptor (citrine) and donor (eCFP) fluorescence ($R=F_A/F_D$; **Figure 3B,C**). This ratio is typically used as a proxy for relative intracellular Ca^{2+} concentration, but after calibration (see 3.3), also absolute concentrations can be estimated (see 3.4.3).
      Note: The pedicles can be recognized by their location in the outer plexiform layer and their morphology (somewhat flattened "blobs" smaller than the cone somata, located at the end of the cone axon).
   2. Average stimulus trials (**Figure 4A**). Extract response parameters from averaged traces (**Figure 4B**), such as Ca^{2+} baseline level (R_{base}) prior to light stimulation, peak amplitude (R_{amp}), and area under the curve (R_A) as measures for response size. Also, extract response kinetics from averaged traces, such as response rise (t_{rise}) and decay time (t_{decay}) (= respective time intervals between 20% and 80% of R_{amp}; see illustration in **Figure 4B**). For more details on how to determine these parameters, see[10].
   3. Calculate an estimate of the absolute cone Ca^{2+} concentration based on the measurements from steps 3.3.1-3.3.3. Use the ratios for minimal and maximal Ca^{2+} concentration, R_{min} and R_{max}, respectively, the donor fluorescence in the Ca^{2+}-bound ($F_{D,Ca-bound}$) and -unbound ($F_{D,Ca-free}$) state, as well as the *in-vivo* dissociation constant ($K_d = 0.77$, see[16]) for TN-XL with the following equation (analogue to[27]):

$$[Ca^{2+}] = K_d \frac{R - R_{min}}{R_{max} - R} \cdot \frac{F_{D,Ca-free}}{F_{D,Ca-bound}}$$

Representative Results

By combining vertical slices (**Figure 1**) prepared from HR2.1:TN-XL mouse retina with two-photon imaging (**Figure 2**), we were able to perform ratiometric measurements of light stimulus-evoked Ca^{2+} signals in cone photoreceptor axon terminals. This approach represents a significant improvement in accessing and visualizing mouse cones over the pre-existing optical imaging methods with synthetic Ca^{2+} indicators. For instance, the cone-specific expression of the genetically-encoded ratiometric Ca^{2+} biosensor TN-XL greatly facilitated the identification of cone axon terminals (see ROIs in **Figure 3A**). Therefore, our protocol eliminates the risk of recording signals of unclear origin, as for example "mixed" signals with contributions from both cone and rod axon terminals.

Our approach allows resolving single-trial responses at the level of the individual cone axon terminal. Light-evoked extrusion of Ca^{2+} from the cone terminal is marked by an increase and a decrease in donor and acceptor fluorescence, respectively (**Figure 3B**). Decrease in fluorescence ratio (R) corresponds to the extrusion of Ca^{2+} from the cone terminal (**Figure 3C**), caused by the light-induced hyperpolarization of the cone and subsequent closure of voltage-gated Ca^{2+} channels. Because several cone axon terminals can be monitored simultaneously (**Figure 3A**), data acquisition is very efficient and hundreds of cone Ca^{2+} responses can be collected in a single experiment. By assessing these responses quantitatively (**Figure 4**), cone Ca^{2+} signals can be compared and evaluated in a range of conditions (see Discussion).

It is often sufficient to use the ratio between FRET-acceptor (citrine) and -donor (eCFP) fluorescence (F_A/F_D; for details, see 3.4) as a relative measure of the intracellular Ca^{2+} level. Yet, whenever necessary, the ratio can be calibrated to obtain absolute intracellular Ca^{2+} concentrations ($[Ca^{2+}]$) (**Figure 5**). At the background illumination used in this protocol (for details, see[10] and **Figure 3** legend), calibration yielded an estimate for the absolute resting $[Ca^{2+}]$ in "wild-type" HR2.1:TN-XL mouse cone terminals of 243 ± 159 nM (mean ± S.D.), which is within the range reported for mice in the literature[11].
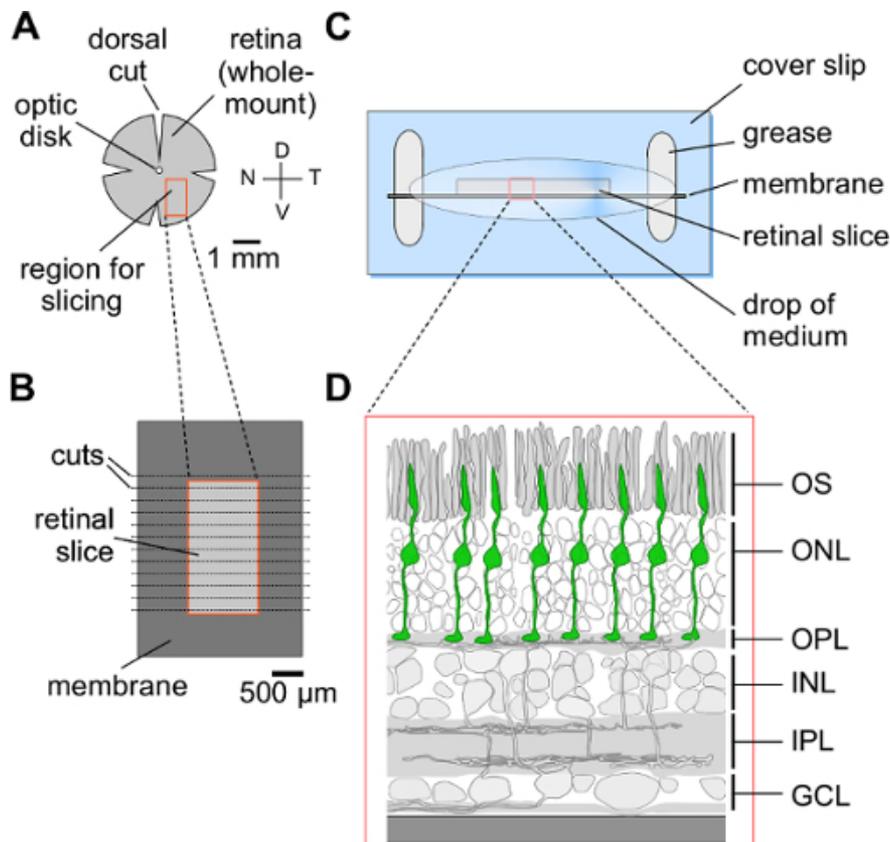
Figure 1. Preparation of vertical retinal slices. (A) Isolated and flattened retina prepared for slicing. **(B)** Rectangular piece of retina (see red box in A) mounted on filter paper membrane (dark grey) after slicing. **(C)** Top view of the membrane-mounted retinal slice fixed on a glass coverslip using grease. **(D)** Schematic drawing of a part of a retinal slice (see red box in C). Cone photoreceptors are indicated in green. V, ventral; D, dorsal; N, nasal; T, temporal; OS, outer segment; ONL, outer nuclear layer; OPL, outer plexiform layer; INL, inner nuclear layer; IPL, inner plexiform layer; GCL, ganglion cell layer. Please click here to view a larger version of this figure.
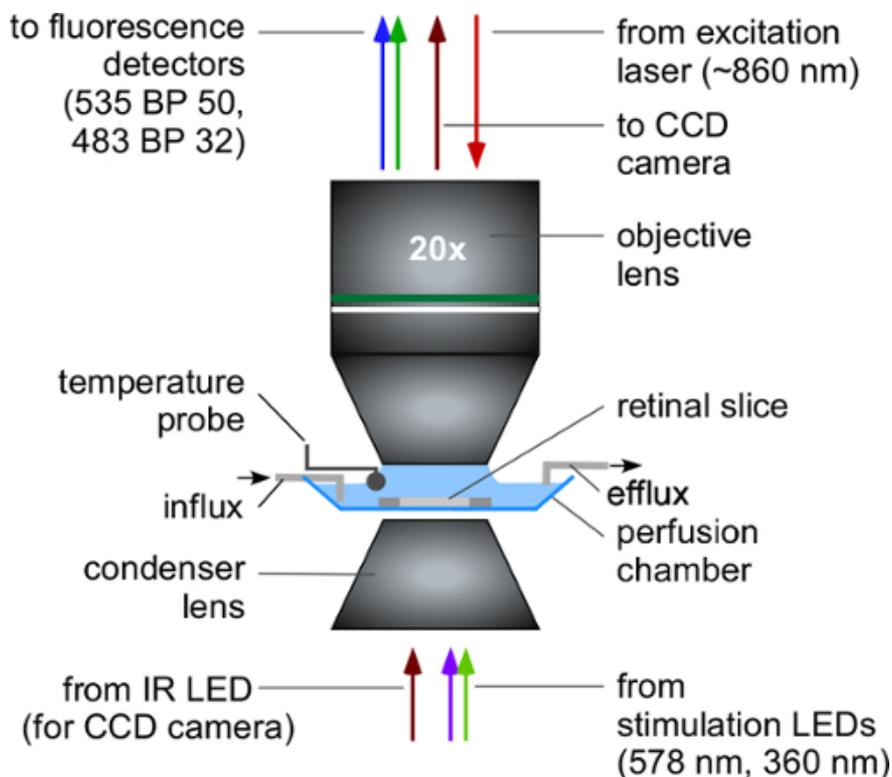
Figure 2. Two-photon imaging of retinal slices: Illustration of the recording configuration. *Top*: Water-immersion objective lens focusing the beam of the scanning laser (red downward arrow) into the retina, and collecting the emitted fluorescence (upward arrows). The lens also collects transmitted infrared light from an illumination LED mounted below the condenser when imaging the slice using a CCD camera. *Center*: Retinal slice mounted in the recording chamber and perfused with extracellular solution. *Bottom*: Condenser lens focusing the light from the stimulation LEDs (and the infrared LED for CCD camera imaging) through the transparent bottom of the recording chamber into the retinal tissue. IR LED, infrared light-emitting diode; CCD, charge-coupled device; BP, band-pass. Please click here to view a larger version of this figure.

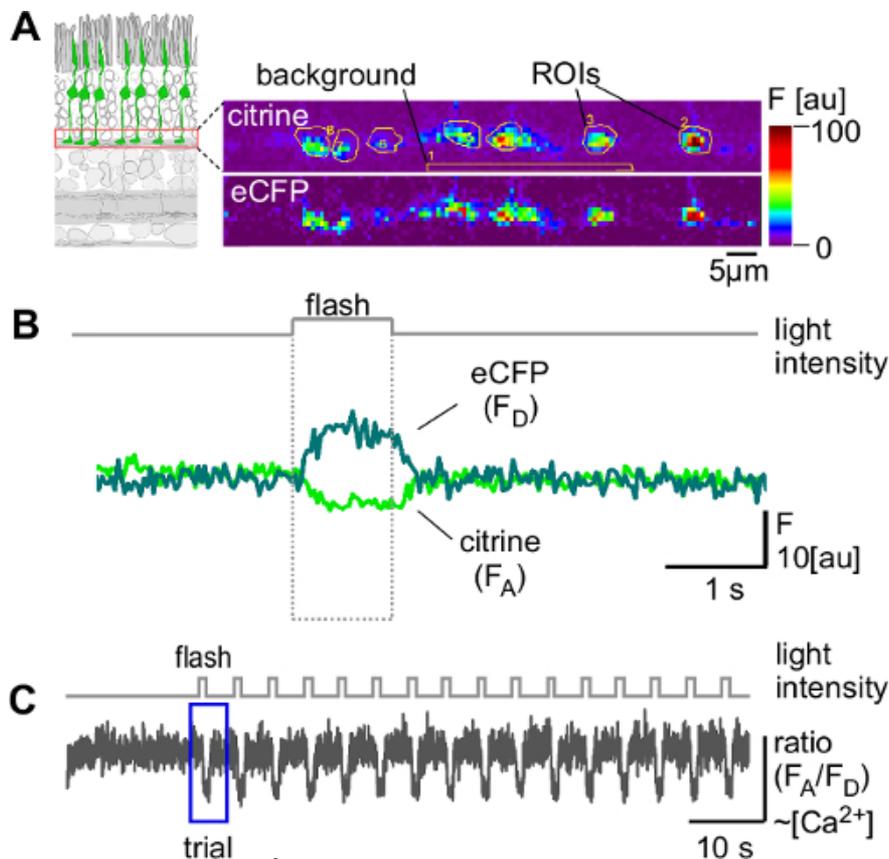**Figure 3. Light-evoked Ca²⁺ responses in axon terminals of mouse cone photoreceptors. (A)** *Left*: Recordings focused on synaptic terminals (red box) of cone photoreceptors (green) in retinal slices. *Right:* Example for a recorded region with 7 individual terminals. Fluorescence was recorded using two channels: one for the FRET-acceptor citrine (top; 535 BP 50) and one for the FRET-donor eCFP (bottom; 480 BP 32). **(B)** Light-evoked changes in citrine (F_A) and eCFP (F_D) fluorescence recorded in a single ROI. **(C)** Ca²⁺ responses (as ratio F_A/F_D) of a cone terminal to a series of 1 sec bright light flashes in 5 sec intervals. ROI, region of interest; BP, band-pass filter; F, fluorescence intensity; a.u., arbitrary units; FRET, Förster resonance energy transfer; eCFP, enhanced cyan fluorescence protein. Stimulus intensity (as photo-isomerization rate in $10^3 \cdot P \cdot s^{-1}$ per cone): 13.0 and 12.8 for M- and S-opsins, respectively, adding onto a background level (= LEDs off, excitation laser scanning) of ~10. Please click here to view a larger version of this figure.
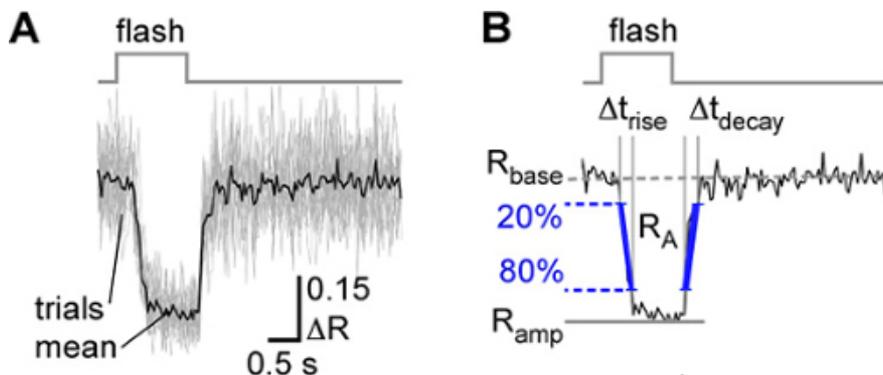

Figure 4. Exemplary quantitative analysis of light-evoked cone Ca²⁺ responses. (A) Light-evoked Ca²⁺ responses (as ΔR) from a single cone terminal (single trials: grey traces, n=16; mean: black trace). **(B)** Parameters determined for the mean Ca²⁺ response: Resting Ca²⁺ level (R_{base}) representing the baseline prior to light stimulation, response size as area-under-the-curve (R_A) and peak amplitude (R_{amp}), kinetics of response onset (t_{rise}, time interval from 20% to 80% of R_{amp}) and offset (t_{decay}, time interval from 80% to 20% of R_{amp}). Please click here to view a larger version of this figure.
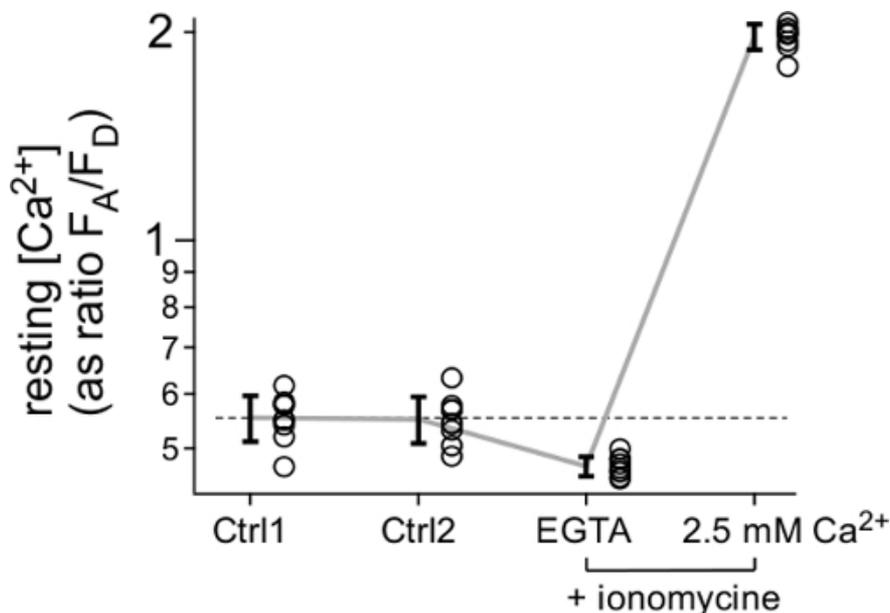
Figure 5. Estimating absolute Ca²⁺ concentration. Resting Ca²⁺ concentration ($[Ca^{2+}]$, as ratio F_A/F_D) recorded in 8 cone axon terminals in a TN-XL mouse (circles, with mean ± S.D.) for different extracellular solutions: twice in standard extracellular medium (Ctrl 1 and 2), then with minimal ("zero") $[Ca^{2+}]$ (10 mM EGTA) and with high $[Ca^{2+}]$ (2.5 mM), the latter two conditions in the presence of 5 µM ionomycin to equilibrate extracellular and intracellular Ca²⁺. Please click here to view a larger version of this figure.

Discussion

Pre-existing protocols using electrophysiological single-cell recordings or Ca²⁺ imaging with synthetic fluorescent indicators struggle to record the Ca²⁺ dynamics in mouse cone photoreceptors for a number of technical reasons (see Introduction). The protocol described here allows the measurement of Ca²⁺ signals and even absolute Ca²⁺ levels in individual, identified mouse cone terminals in an efficient and relatively simple way.

This protocol has already been successfully used in three studies addressing different aspects of cone function in healthy mouse retina. In the first study[10], the HR2.1:TN-XL mouse was characterized using immunohistochemistry, ERG recordings, two-photon Ca²⁺ imaging, and pharmacology, showing that the cone-specific expression of the Ca²⁺ biosensor does not hamper cone anatomy and function. In the second study[21], chromatic and achromatic response properties of mouse cones were mapped across the retina, demonstrating striking differences in cone function between the "green" opsin-dominated dorsal and the "blue" opsin-dominated ventral mouse retina. These regional differences in cone properties matched the differential contrast distribution in the natural environment (*i.e.*, sky *vs.* ground), suggesting that the different spectral types of mouse cones provide for (near) optimal sampling of achromatic contrasts and, thus, may offer an evolutionary advantage. In the third study[22] the reciprocal feedback that cone axon terminals receive from horizontal cells was investigated. As all proposed horizontal cell feedback mechanisms act on voltage-gated Ca²⁺ channels in the cone axon terminals[28], cone terminal Ca²⁺ can serve as a proxy for horizontal cell-to-cone interactions. The study by Kemmler and coworkers[22] supports the view that horizontal cells use a complex feedback system comprising several mechanisms to control photoreceptor glutamate release.

These studies illustrate the versatility of the described protocol and show that it can be adapted to a wide range of questions concerning cone function and its synaptic circuits. In addition, the protocol enables studying local Ca²⁺ signaling in the different cone compartments, towards a better comprehension of cone physiology. Such knowledge is important to understand pathophysiological processes in degenerating cones, to eventually allow for the rational development of potential therapeutic approaches, in particular for degenerative diseases affecting cones.

In the HR2.1:TN-XL mouse line, the Ca²⁺ biosensor is expressed throughout the cone, with the exception of the outer segment. This provides an opportunity for direct and ratiometric assessment of Ca²⁺ dynamics in different cone compartments. Since changes in Ca²⁺ currents in the outer segment are reflected in terminals *via* the membrane potential and the resulting activation of voltage-gated Ca²⁺ channels, processes in the outer segment can be observed indirectly.

Potential pitfalls:

The dissection of the retina is a critical step: In the mouse, the retina separates from the eyecup usually between photoreceptor outer segments and pigment epithelium. Therefore, the light-sensitive photoreceptor outer segments of the isolated retina are exposed and extremely sensitive to mechanical damage. Great care must be taken not to damage by touching the photoreceptor side with tools or by moving the tissue sideways on an adhesive surface (*e.g.,* a filter membrane).

High-quality retinal slices can be recognized under the microscope by their clean cutting surface and by a well-organized photoreceptor layer with clearly defined outer segments. Functional assessment of slice quality can be quickly done by flashing bright light stimuli and determining the percentage of responsive cones (*e.g.*, in a field of view with 10 - 20 cones). Here, response quality should be evaluated by calculating the signal-to-noise ratio (S/N) (amplitude of baseline noise before the light stimulus *vs.* amplitude of the light response); a S/N of 2 - 3 should be

considered as the minimum threshold. Typically, we discard slices with less than 50% responsive cones. Also slices with cones that display excessive spontaneous spiking behaviour (see **Figure 4** in[10]) should be discarded.

Slices in the recording chamber that meet the aforementioned anatomical and functional criteria show consistent responses for 1 - 2 hr (for details on response consistency, see[10]). Because slices survive for hours in the holding chamber, a successful experiment can last up to 6 hr. It is noteworthy that there are some restrictions with respect to studying long-ranging spatial interactions between cones and horizontal cells, as slicing inevitably severs lateral connections in retinal networks. However, increasing the thickness of retinal slices to 300 µm ameliorates this issue[22].

The use of vertical retinal slices avoids scanning of light-sensitive cone outer segments by the excitation laser and, thus, largely prevents opsin bleaching (for extensive discussion, see[10,21]). Nevertheless, the recorded Ca^{2+} signals not only depend on the light stimuli, but also get affected by a background illumination component generated by the scanning excitation laser. In fact, the effective background illumination in such two-photon imaging experiments is a combination of scattered laser light, fluorescent light emitted by the recorded cells, and any LED stimulus background component. Therefore, cones should be allowed to adapt for at least 20 - 30 s to laser scanning (with the background component of the light stimulus turned on) prior to recording.

Advantages and applications:

While some applications for this cone Ca^{2+}-imaging protocol have been described above[10,21,22], other applications can be envisioned: Pharmacological studies in combination with cone Ca^{2+} imaging may validate Ca^{2+} signaling pathways in cones and could be used to test efficacy and potency of drugs targeting different players in Ca^{2+}-signaling[10]. However, a key application may be to study diseases affecting cone function. Many retinal degeneration mouse models mimicking human diseases are available. For instance, the cone photoreceptor loss 1 (*cpfl*1) mouse is a primary cone degeneration model suffering from a *Pde6c* mutation[29]. Conversely, the rod degeneration 1 (*rd*1) mouse suffers from a *Pde6b* mutation. While this causes primary rod photoreceptor degeneration[30], once *rd*1 rod loss is completed, secondary cone degeneration sets in[1]. Crossbreeding these animals with the HR2.1:TN-XL line will allow studying and comparing Ca^{2+} dynamics in both primary and secondary cone degeneration and is likely to provide valuable insights into the role of Ca^{2+} during cone cell death. Also, pharmacologically induced cone degeneration – for instance using selective PDE6 inhibitors – may serve to identify the downstream mechanisms of cone degeneration[10,29,31].

In summary, the protocol described here allows measuring Ca^{2+} in subcellular compartments of mouse cone photoreceptors and presents great opportunities to uncover cone physiology under a wide range of physiological and pathophysiological conditions. Additionally, this protocol may be used for the screening of pharmacological agents designed to interfere with cone Ca^{2+}-signaling and thus help to establish new therapies for cone diseases.

Disclosures

The authors have nothing to disclose.

Acknowledgements

References

1. Trifunovic, D., *et al.* Neuroprotective strategies for the treatment of inherited photoreceptor degeneration. *Current Molecular Medicine.* **12**, 598-612 (2012).
2. Paquet-Durand, F., *et al.* Calpain is activated in degenerating photoreceptors in the rd1 mouse. *Journal of Neurochemistry.* **96**, 802-814 (2006).
3. Paquet-Durand, F., *et al.* A key role for cyclic nucleotide gated (CNG) channels in cGMP-related retinitis pigmentosa. *Human Molecular Genetics.* **20**, 941-947 (2011).
4. Frasson, M., *et al.* Retinitis pigmentosa: rod photoreceptor rescue by a calcium-channel blocker in the rd mouse. *Nature Medicine.* **5**, 1183-1187 (1999).
5. Bush, R. A., Kononen, L., Machida, S., Sieving, P. A. The effect of calcium channel blocker diltiazem on photoreceptor degeneration in the rhodopsin Pro213His rat. *Investigative Ophthalmology & Visual Science.* **41**, 2697-2701 (2000).
6. Pawlyk, B. S., Li, T., Scimeca, M. S., Sandberg, M. A., Berson, E. L. Absence of photoreceptor rescue with D-cis-diltiazem in the rd mouse. *Investigative Ophthalmology & Visual Science.* **43**, 1912-1915 (2002).
7. Sampath, A. P., Matthews, H. R., Cornwall, M. C., Bandarchi, J., Fain, G. L. Light-dependent changes in outer segment free-Ca2+ concentration in salamander cone photoreceptors. *The Journal of General Physiology.* **113**, 267-277 (1999).
8. Choi, S. Y., *et al.* Encoding light intensity by the cone photoreceptor synapse. *Neuron.* **48**, 555-562 (2005).
9. Krizaj, D. Calcium stores in vertebrate photoreceptors. *Advances in Experimental Medicine and Biology.* **740**, 873-889 (2012).
10. Wei, T., *et al.* Light-driven calcium signals in mouse cone photoreceptors. *The Journal of Neuroscience.* **32**, 6981-6994 (2012).
11. Johnson, J. E. Jr, *et al.* Spatiotemporal regulation of ATP and Ca2+ dynamics in vertebrate rod and cone ribbon synapses. *Molecular Vision.* **13**, 887-919 (2007).
12. Jeon, C. J., Strettoi, E., Masland, R. H. The major cell populations of the mouse retina. *The Journal of Neuroscience.* **18**, 8936-8946 (1998).
13. Palmer, A. E., Tsien, R. Y. Measuring calcium signaling using genetically targetable fluorescent indicators. *Nature Protocols.* **1**, 1057-1065 (2006).
14. Paredes, R. M., Etzler, J. C., Watts, L. T., Zheng, W., Lechleiter, J. D. Chemical calcium indicators. *Methods.* **46**, 143-151 (2008).

15. Tsien, R. Y. A non-disruptive technique for loading calcium buffers and indicators into cells. *Nature.* **290**, 527-528 (1981).

16. Hendel, T., *et al.* Fluorescence changes of genetic calcium indicators and OGB-1 correlated with neural activity and calcium in vivo and in vitro. *The Journal of Neuroscience.* **28**, 7399-7411 (2008).

17. Dreosti, E., Odermatt, B., Dorostkar, M. M., Lagnado, L. A genetically encoded reporter of synaptic activity in vivo. *Nature Methods.* **6**, 883-889 (2009).

18. Mank, M., *et al.* A FRET-based calcium biosensor with fast signal kinetics and high fluorescence change. *Biophysical Journal.* **90**, 1790-1796 (2006).

19. Wang, Y., *et al.* A locus control region adjacent to the human red and green visual pigment genes. *Neuron.* **9**, 429-440 (1992).

20. Connaughton, V. P. Zebrafish retinal slice preparation. *Methods in Cell Science.* **25**, 49-58 (2003).

21. Baden, T., *et al.* A tale of two retinal domains: near-optimal sampling of achromatic contrasts in natural scenes through asymmetric photoreceptor distribution. *Neuron.* **80**, 1206-1217 (2013).

22. Kemmler, R., Schultz, k, Dedek, K., Euler, T., Schubert, T. Differential regulation of cone calcium signals by different horizontal cell feedback mechanisms in the mouse retina. *The Journal of Neuroscience.* **34**, 11826-11843 (2014).

23. Werblin, F. S. Transmission along and between rods in the tiger salamander retina. *The Journal of Physiology.* **280**, 449-470 (1978).

24. Euler, T., *et al.* Eyecup scope--optical recordings of light stimulus-evoked fluorescence signals in the retina. Pflugers Archive. *European Journal of Physiology.* **457**, 1393-1414 (2009).

25. Baden, T., Berens, P., Bethge, M., Euler, T. Spikes in mammalian bipolar cells support temporal layering of the inner retina. *Current Biology.* **23**, 48-52 (2013).

26. Breuninger, T., Puller, C., Haverkamp, S., Euler, T. Chromatic bipolar cell pathways in the mouse retina. *The Journal of Neuroscience.* **31**, 6504-6517 (2011).

27. Grynkiewicz, G., Poenie, M., Tsien, R. Y. A new generation of Ca2+ indicators with greatly improved fluorescence properties. *The Journal of Biological Chemistry.* **260**, 3440-3450 (1985).

28. Thoreson, W. B., Mangel, S. C. Lateral interactions in the outer retina. *Progress in Retinal and Eye Research.* **31**, 407-441 (2012).

29. Trifunovic, D., *et al.* cGMP-dependent cone photoreceptor degeneration in the cpfl1 mouse retina. *The Journal of Comparative Neurology.* **518**, 3604-3617 (2010).

30. Sahaboglu, A., *et al.* Retinitis pigmentosa: rapid neurodegeneration is governed by slow cell death mechanisms. *Cell Death & Disease.* **4**, e488 (2013).

31. Sahaboglu, A., *et al.* PARP1 gene knock-out increases resistance to retinal degeneration without affecting retinal function. *PloS One.* **5**, e15495 (2010).